

# Fourier Transform IR Spectra and Rovibrational Investigation of Monoisotopic $\text{H}_3^{116}\text{Sn}^{35}\text{Cl}$ , $\text{H}_3^{116}\text{Sn}^{79}\text{Br}$ and $\text{H}_3^{116}\text{SnI}$ in the $\nu_6$ Region

M. Betzel, H. Bürger, and A. Rahner

FB 9 – Anorganische Chemie, Universität – Gesamthochschule, Wuppertal, West Germany

Z. Naturforsch. **41 a**, 1009–1014 (1986); received April 1, 1986

Fourier transform infrared spectra in the  $\nu_6$  region of the unstable monoisotopic species  $\text{H}_3^{116}\text{Sn}^{35}\text{Cl}$ ,  $\text{H}_3^{116}\text{Sn}^{79}\text{Br}$  and  $\text{H}_3^{116}\text{SnI}$  have been recorded with a resolution of  $0.04\text{ cm}^{-1}$  ( $0.12\text{ cm}^{-1}$  for  $\text{H}_3\text{SnI}$ ). Rotational  $J$  and  $K$  structure of the  $\nu_6$  fundamental has been resolved for  $\text{H}_3\text{SnCl}$  and  $\text{H}_3\text{SnBr}$ , while  $Q$  branches were measured for  $\text{H}_3\text{SnI}$ . The hot bands  $(\nu_3 + \nu_6) - \nu_3$  and  $2\nu_6^{\pm 2} - \nu_6^{\pm 1}$  have been identified. A rovibrational analysis has been performed, and the following band centers (for given  $A_0$  values) have been determined:  $\text{H}_3^{116}\text{Sn}^{35}\text{Cl}$   $488.786(2)$ ,  $\text{H}_3^{116}\text{Sn}^{79}\text{Br}$   $473.493(2)$  and  $\text{H}_3^{116}\text{SnI}$   $453.680(9)\text{ cm}^{-1}$ .

## 1. Introduction

In previous contributions from our laboratory we have reported the first unambiguous detection by infrared spectroscopy of the unstable stannyl halides  $\text{H}_3\text{SnCl}$ ,  $\text{H}_3\text{SnBr}$  and  $\text{H}_3\text{SnI}$  [1, 2]. Employing monoisotopic species,  $J$  structure of the  $\nu_3$  band has been resolved, and a rotational analysis has been performed [2]. Furthermore, the  $\nu_1/\nu_4$  pair of  $\text{H}_3^{116}\text{Sn}^{35}\text{Cl}$  near  $1900\text{ cm}^{-1}$  involved in Coriolis  $x, y$  resonance has been identified in spite of the difficulties encountered by the overlap with strong  $\text{SnH}_4$  absorptions unevitably present in this region of the spectrum.

The rotational analysis of the fundamentals  $\nu_1/\nu_4$  near  $1900\text{ cm}^{-1}$  and  $\nu_2/\nu_5$  near  $700\text{ cm}^{-1}$  requires a secure knowledge of the low-lying fundamentals  $\nu_3$  and  $\nu_6$  because multiply excited states involving  $\nu_3$  and  $\nu_6$  quanta may interact with  $\nu_1/\nu_4$  and  $\nu_2/\nu_5$  by different coupling mechanisms as has been shown for the lighter methyl, silyl and germyl homologues. In proceeding with the rotational analysis of the fundamental vibrations of the stannyl halides, we therefore deal in the present study with the lowest-lying perpendicular fundamental  $\nu_6$  which is associated with the  $\text{SnH}_3$  rocking mode.

The stannyl halides are short-lived species decomposing in the gas phase at  $0^\circ\text{C}$  within minutes. A major complication is the fact that tin is

the element with the greatest number of naturally occurring isotopes. Thus the use of rigorously monoisotopic samples is compulsory if a measurement of lines is intended. We have chosen for this purpose as pilot isotope  $^{116}\text{Sn}$ , natural abundance 14.24%, as well as  $^{35}\text{Cl}$  and  $^{79}\text{Br}$ , natural abundances 75.5 and 50.5% respectively. The low quantity of isotopically enriched samples available and the rapid decomposition of the stannyl halides upon condensation prohibited the use of continuous flow techniques and employment of large cells with great path lengths. Considering the limited measuring time available, the relatively low intensity of the  $\nu_6$  fundamental lowered the quality of the spectra, and a further limit was given by the available resolution ( $4 \times 10^{-2}\text{ cm}^{-1}$ ). In spite of these difficulties we were able to detect for the first time the  $\nu_6$  fundamental of the stannyl halides and to unambiguously assign rotational features. In the present contribution (part LIII, for part LII of this series cf. [3]) we report on our results.

## 2. Experimental

The synthesis of the monoisotopic species has been described previously [2]. A double-jacketed 17 cm stainless steel cell equipped with KBr windows was employed, cold  $\text{N}_2$  being used to adjust the temperature between  $-5$  and  $0^\circ\text{C}$ . The total pressure in the cell was of the order of 10 mbar. A Nicolet Series 8000 vacuum interferometer achiev-

Reprint requests to Prof. Dr. H. Bürger, Universität – Gesamthochschule, Gaußstraße 20, D-5600 Wuppertal 1.

0340-4811 / 86 / 0800-1009 \$ 01.30/0. – Please order a reprint rather than making your own copy.



Dieses Werk wurde im Jahr 2013 vom Verlag Zeitschrift für Naturforschung in Zusammenarbeit mit der Max-Planck-Gesellschaft zur Förderung der Wissenschaften e.V. digitalisiert und unter folgender Lizenz veröffentlicht: Creative Commons Namensnennung-Keine Bearbeitung 3.0 Deutschland Lizenz.

Zum 01.01.2015 ist eine Anpassung der Lizenzbedingungen (Entfall der Creative Commons Lizenzbedingung „Keine Bearbeitung“) beabsichtigt, um eine Nachnutzung auch im Rahmen zukünftiger wissenschaftlicher Nutzungsformen zu ermöglichen.

This work has been digitalized and published in 2013 by Verlag Zeitschrift für Naturforschung in cooperation with the Max Planck Society for the Advancement of Science under a Creative Commons Attribution-NoDerivs 3.0 Germany License.

On 01.01.2015 it is planned to change the License Conditions (the removal of the Creative Commons License condition “no derivative works”). This is to allow reuse in the area of future scientific usage.

ing an unapodized resolution of  $0.04 \text{ cm}^{-1}$  was used. It was equipped with a  $3 \mu$  mylar beam splitter, and a Cu:Ge detector operating at  $4.2 \text{ K}$  was used. Measuring times on the order of 5 to 15 min were available before complete decomposition of the samples was noted, and blocks of interferograms were collected consecutively and examined later. Calibration was with  $\text{H}_2\text{O}$  rotational lines [4]; the absolute wavenumber accuracy of peakfinder-evaluated lines is better than  $\pm 2 \times 10^{-3} \text{ cm}^{-1}$ .

### 3. General

The  $\nu_6$  fundamental of the stannyl halides is similar to that of the silyl and, in particular, germlyl halides  $\text{H}_3\text{GeCl}$  [5],  $\text{H}_3\text{GeBr}$  [6] and  $\text{H}_3\text{GeI}$  [7], all of which are prolate symmetric tops with a large  $A:B$  ratio. For details the reader is referred to [5–7].

The spectra comprise unresolved, strong  $Q$  branches with alternating intensity, which are accompanied by hot bands, and rotational lines. The intensities of the most prominent hot bands at  $270 \text{ K}$  relative to the cold bands are as follows:

	$(\nu_3 + \nu_6) - \nu_3$	$2\nu_6^{\pm 2} - \nu_6^{\pm 1}$	$2\nu_6^0 - \nu_6^{\pm 1}$
$\text{H}_3^{116}\text{Sn}^{35}\text{Cl}$	0.14	0.16	0.08
$\text{H}_3^{116}\text{Sn}^{79}\text{Br}$	0.24	0.17	0.08
$\text{H}_3^{116}\text{SnI}$	0.33	0.19	0.09

The intensity alternation due to hydrogen nuclear spin gives double intensity to transitions of  $\nu_6$  and  $(\nu_3 + \nu_6) - \nu_6$  with  $K'' = 3p$ ,  $p = 0, 1, 2, 3, \dots$ , while double intensity for  $K'' = 3p \pm 1$  is associated with  $\Delta K = \pm 1$  transitions of  $2\nu_6^{\pm 2} - \nu_6^{\pm 1}$  and  $\Delta K = \mp 1$  transitions of  $2\nu_6^0 - \nu_6^{\pm 1}$ .

Since no lines due to the hot bands could be assigned with certainty, relative displacements of  $Q$  branch edges of  $(\nu_3 + \nu_6) - \nu_3$  and  $2\nu_6^{\pm 2} - \nu_6^{\pm 1}$  from  $\nu_6$  were determined by polynomial methods, Table 3. From these displacements  $x_{36}$  and  $(x_{66} + g_{66})$  were determined using the appropriate formulae. Since the hot band  $(2\nu_6^0 - \nu_6^{\pm 1})$  appeared to be buried under the  $Q$  branches of  $\nu_6$ , as was also observed for the germlyl halides [5–7], the quantity  $(x_{66} - g_{66})$  and hence  $x_{66}$  and  $g_{66}$  could not be determined.

Excited state parameters of  $\nu_6$  of  $\text{H}_3^{116}\text{Sn}^{35}\text{Cl}$  and  $\text{H}_3^{116}\text{Sn}^{79}\text{Br}$  were determined from individual rotational lines which, for a fixed ground state

$$E_0(J, K) = (A_0 - B_0) K^2 + B_0 J(J+1) - D_J^0 J^2(J+1)^2 - D_{JK}^0 J(J+1) K^2 - D_K^0 K^4 \quad (1)$$

were fitted to excited state energies

$$E_6(v_6, l_6, J, k) = v_6^0 + (A_6 - B_6) k^2 + B_6 J(J+1) - D_J^6 J^2(J+1)^2 - D_{JK}^6 J(J+1) k^2 - D_K^6 k^4 - [2A \zeta_6 - \eta_{6J} J(J+1) - \eta_{6K} k^2] k l_6. \quad (2)$$

Perturbations due to  $\Delta l = \Delta k = \pm 2$  interactions affecting the  $k l = 1$  sublevels were accounted for by an off-diagonal element:

$$\begin{aligned} \langle v_6 = 1, l_6 = +1, J, k+1 | H | v_6 = 1, l_6 = -1, J, k-1 \rangle \\ = -2F_6 [J(J+1) - k(k+1)]^{1/2} \\ \cdot [J(J+1) - k(k-1)]^{1/2} \end{aligned} \quad (3)$$

with the sign convention of [8],  $q_6^+ = 4F_6$ .

The least squares program MILLI [9] was used for the numerical treatment of the data. For  $\text{H}_3^{116}\text{SnI}$  we proceeded in a different way. Due to the smallness of  $B_0$ ,  $0.038 \text{ cm}^{-1}$ , the extensive population of vibrationally excited levels at  $270 \text{ K}$  and the overlap of  $J$  systems belonging to different  $K$  values, the interferometer available to us did not permit resolution of rotational  $J$  structure. Therefore this structure was fully suppressed by measuring the spectra with a resolution of  $0.12 \text{ cm}^{-1}$ .  $Q$  branch edges were treated as first  $Q$  branch lines [ ${}^R Q_K(J = K+1)$ ,  ${}^P Q_K(J = K)$ ] with  $(B_6 - B_0)$  determined by band contour simulation. Clearly a larger uncertainty has to be ascribed to the excited state parameters, in particular  $v_6^0$ , of  $\text{H}_3\text{SnI}$ .

## 4. Rovibrational Analysis

### 4.1 Ground State

Some ground state constants, Table 1, are available from mw measurements [10–12]. Further data come from the  $\nu_3$  analysis [2], while parameters not otherwise accessible were computed by a harmonic force field ( $D^0$ 's) or deduced from the predicted geometry ( $A_0$ ). The quantities not directly measured and the values to which they are related ( $v_0, A \zeta^z, \eta_J, \eta_K$ ) should be considered with great caution.

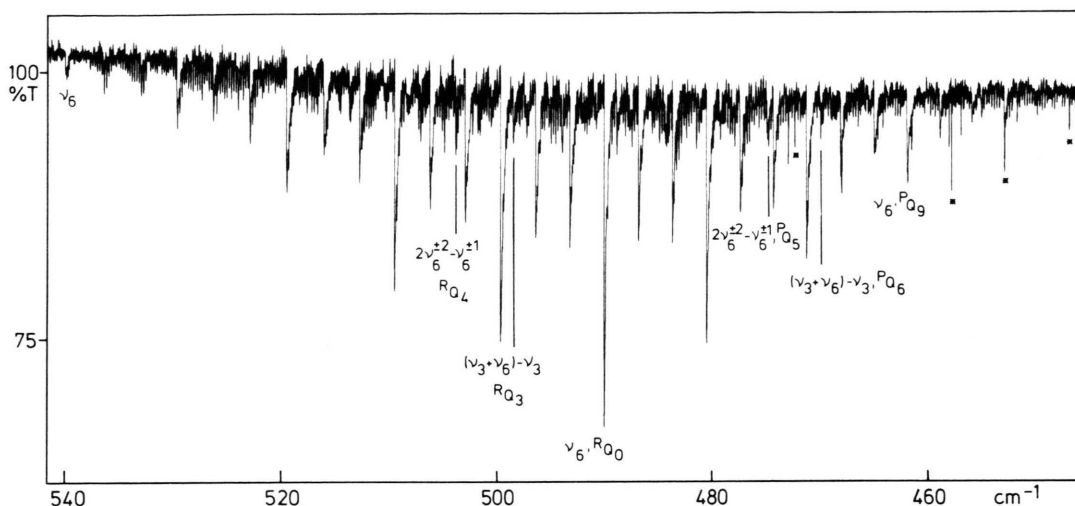


Fig. 1. Survey spectrum of  $\text{H}_3^{116}\text{Sn}^{35}\text{Cl}$  in the  $\nu_6$  region. Resolution  $0.04\text{ cm}^{-1}$ . Some  $Q$  branches of  $\nu_6$ ,  $(\nu_3 + \nu_6) - \nu_3$  and  $2\nu_6^{\pm 2} - \nu_6^{\pm 1}$  are assigned. Lines marked with an asterisk are due to  $\text{H}_2\text{O}$ .

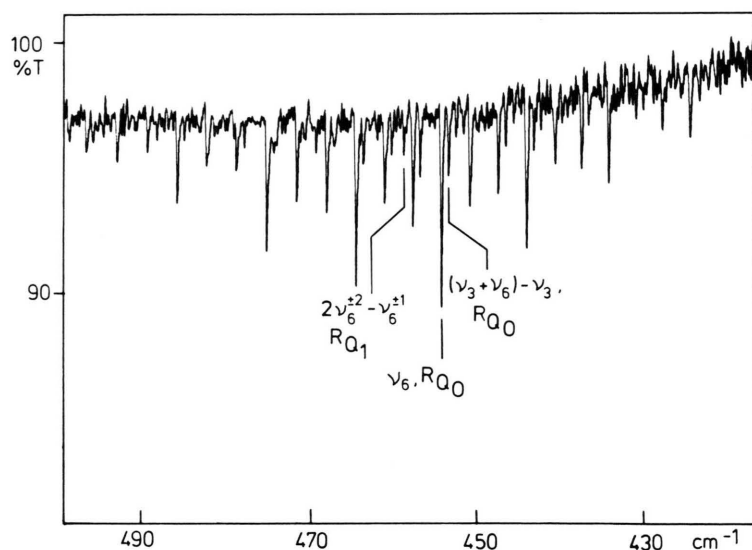


Fig. 2. Survey spectrum of  $\text{H}_3^{116}\text{SnI}$  in the  $\nu_6$  region. Resolution  $0.12\text{ cm}^{-1}$ . Some assignments are given.

Table 1. Ground state constants of stannyl halides ( $\text{cm}^{-1}$ ).

	$\text{H}_3^{116}\text{Sn}^{35}\text{Cl}$	$\text{H}_3^{116}\text{Sn}^{79}\text{Br}$	$\text{H}_3^{116}\text{SnI}$
$A_0$	2.12 <sup>a</sup>	2.11 <sup>a</sup>	2.10 <sup>a</sup>
$B_0$	0.110 431 [10]	0.056 746 9 [11]	0.037 614 7 [12]
$D_J^0 \times 10^8$	3.51 <sup>b</sup>	1.02 [2]	0.477 [2] <sup>c</sup>
$D_{JK}^0 \times 10^7$	8.98 <sup>b</sup>	2.30 [11]	1.37 [12]
$D_K^0 \times 10^5$	1.60 <sup>b</sup>	1.615 <sup>b</sup>	1.60 <sup>b</sup>

<sup>a</sup> From estimated structure. — <sup>b</sup> From harmonic force field. — <sup>c</sup>  $4B^3/(\nu_3)^2$ .

## 4.2 Excited States

The spectra of  $\text{H}_3^{116}\text{Sn}^{35}\text{Cl}$  and  $\text{H}_3^{116}\text{SnI}$  are illustrated in Figs. 1 and 2, while a detail of the spectrum of  $\text{H}_3^{116}\text{Sn}^{79}\text{Br}$  together with a band contour simulation neglecting hot bands is shown in Figure 3. The assignment follows from the intensity alternation in connection with the significantly sharper  $^RQ_0$  branch (and hence negative  $F_6$ ) and first lines which are clearly discernible in many cases. Though there are hardly any pure lines, peaks

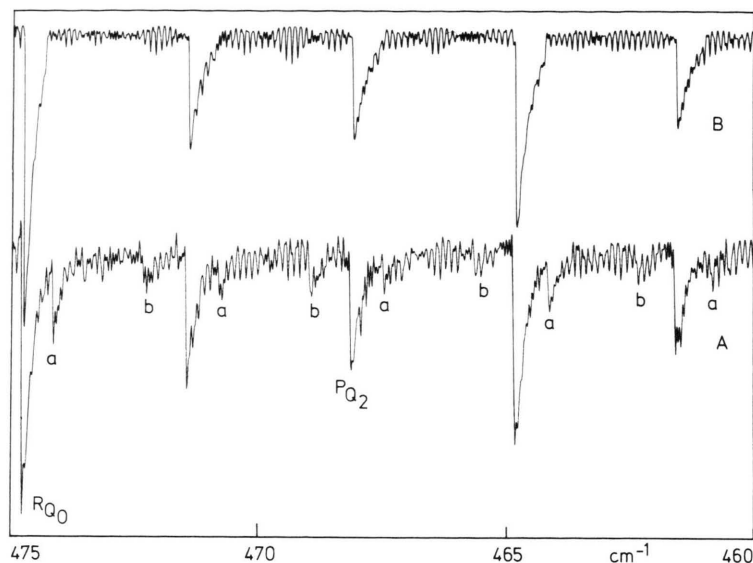


Fig. 3. Detail of the spectrum of  $\text{H}_3^{116}\text{Sn}^{79}\text{Br}$  in the  $\nu_6$  region. A) Experimental spectrum, resolution  $0.04\text{ cm}^{-1}$ . a)  $Q$  branches of  $(\nu_3 + \nu_6) - \nu_3$ ; b)  $Q$  branches of  $2\nu_6^{\pm 2} - \nu_6^{\pm 1}$ . B) Band contour simulation, hot bands omitted.

Table 2. Excited state molecular parameters of stannyl halides ( $\text{cm}^{-1}$ ).

	$\text{H}_3^{116}\text{Sn}^{35}\text{Cl}$	$\text{H}_3^{116}\text{Sn}^{79}\text{Br}$	$\text{H}_3^{116}\text{SnI}$
$\nu_6^0$ <sup>a</sup>	488.785 7(6)	473.492 9(7)	453.680(9)
$(A_6 - A_0) \times 10^3$	9.632(8)	9.849(9)	10.41(13)
$(B_6 - B_0) \times 10^5$	-14.27(3)	-7.00(4)	-3.5 fixed <sup>b</sup>
$A \zeta_6^-$	0.415 15(6)	0.393 75(7)	0.399 8(5)
$\eta_{6J} \times 10^6$	1.60(5)	0.66(7)	0 fixed
$\eta_{6K} \times 10^5$	1.68(12)	1.17(13)	0 fixed
$F_6 \times 10^5$	-1.48(3)	-0.55(4)	0 fixed
No. of data	732	630	34
$\sigma \times 10^3$	8.1	8.4	29.7

<sup>a</sup> See text for dependence on  $A_0$ . — <sup>b</sup> By band contour simulation.

were assigned to their major constituents at the expense of a worse rms deviation of observed and calculated wavenumbers. The fits included 723 and 630 unit-weighted lines for  $\text{H}_3\text{SnCl}$  and  $\text{H}_3\text{SnBr}$ , respectively, and 24  $Q$  branch edges for  $\text{H}_3\text{SnI}$ . Lists with observed and calculated transition wavenumbers and the correlation matrices of free parameters have been deposited as supplementary material [13].

The fits readily converged to the excited state parameters set out in Table 2 with  $\sigma = 8.1$ , 8.4 and  $29.5 \times 10^{-3}\text{ cm}^{-1}$ , respectively. Refinement of excited state centrifugal distortions was physically not

meaningful; therefore they were constrained to their ground state values.

The results of the polynomial analyses of  $Q$  branch edges for  $\nu_6$ ,  $(\nu_3 + \nu_6) - \nu_3$  and  $(2\nu_6^{\pm 2} - \nu_6^{\pm 1})$  are given in Table 3, and the deduced anharmonicity constants are quoted.

## 5. Discussion

The present study unambiguously provides the major rovibrational parameters associated with the  $\nu_6$  fundamental for one isotopic species of stannyl chloride, bromide and iodide. In contrast to the C, Si and Ge homologues, no evidence has yet been found for a monomeric fluoride  $\text{H}_3\text{SnF}$ . The important parameters  $\nu_6^0$  and  $A \zeta_6^-$  are correlated with  $A_0$ , and there is urgent demand for information on that parameter, eventually by application of the  $\zeta$  sum rule or mw investigations of partly deuterated species. Whether perturbation-allowed IR transitions which supply information on  $A_0$  can be observed seems questionable presently due to the experimental difficulties in obtaining spectra and the weakness of perturbations in such heavy molecules.

Combining the results of the present study with those of the  $\nu_3$  analysis [2], some predictions of possible perturbations can be made. These follow from inspection of Table 4. The  $\nu_6$  fundamental is

Table 3. Results of polynomial analyses for hot bands. Fit of  $Q$  branch edges according to  $^{(P,R)}Q_K = a_0 + a_1(K \Delta K) + a_2(K \Delta K)^2$  (cm<sup>-1</sup>)<sup>a</sup>.

		H <sub>3</sub> <sup>116</sup> Sn <sup>35</sup> Cl	H <sub>3</sub> <sup>116</sup> Sn <sup>79</sup> Br	H <sub>3</sub> <sup>116</sup> SnI
$\nu_6$	$a_0$	489.957(5)	474.775(5)	454.954(10)
	$a_1$	3.202 9(4)	3.334 2(5)	3.340 1(10)
	$a_2 \times 10^2$	0.934(7)	0.967(8)	1.028(15)
	$\sigma \times 10^2$	1.5	1.7	3.2
$(\nu_3 + \nu_6) - \nu_3$	$a_0$	488.760(15)	474.113(8)	454.108(12)
	$a_1$	3.218 0(32)	3.356 7(9)	3.351 3(18)
	$a_2 \times 10^2$	1.023(58)	1.008(13)	0.849(34)
	$\sigma \times 10^2$	3.7	2.4	3.2
$2\nu_6^{\pm 2} - \nu_6^{\pm 1}$	$a_0$	490.774(12)	475.641(12)	455.788(26)
	$a_1$	3.232 3(18)	3.369 2(21)	3.383 6(32)
	$a_2 \times 10^2$	0.888(32)	1.016(35)	1.642(70)
	$\sigma \times 10^2$	3.2	3.0	6.2
	$x_{36}$	-1.228(16)	-0.666(10)	-0.853(15)
	$x_{66} + g_{66}$	0.808(7)	0.819(7)	0.741(14)

<sup>a</sup> In many cases better fits were obtained with inclusion of a cubic term.Table 4. Rounded vibrational energy levels of stannyl halides (cm<sup>-1</sup>).

	H <sub>3</sub> <sup>116</sup> Sn <sup>35</sup> Cl	H <sub>3</sub> <sup>116</sup> Sn <sup>79</sup> Br	H <sub>3</sub> <sup>116</sup> SnI
$\nu_3$	375.5	263.6	209.8
$2\nu_3$	748.7	525.9	418.7
$3\nu_3$	1 119.7	787.1	626.8
$\nu_6$	488.8	473.5	453.7
$2\nu_6$ av.	978	947	907
$\nu_3 + \nu_6$	863.0	736.4	662.6
$\nu_2$ [14]	694.7	686.7	676.1
$\nu_5$ [14]	702.3	702.6	703.9

expected to be unperturbed, the crossing with  $2\nu_3$  occurring for larger  $K$  values is than relevant in the present study. For H<sub>3</sub><sup>116</sup>Sn<sup>35</sup>Cl, it can be predicted that  $2\nu_3$  and  $\nu_5$  will exhibit a local rotational resonance near  $K$ ,  $(k-l)=10$ , similar to that reported for H<sub>3</sub>C<sup>35</sup>Cl [15]. In H<sub>3</sub>SnBr, a Fermi resonance between  $\nu_5$  and  $\nu_3 + \nu_6$  similar to that reported for H<sub>3</sub>SiI [16] and H<sub>3</sub>GeBr [17] is predict-

ed, which shifts the  $\nu_3 + \nu_6$  level to greater wavenumbers and hence increases the effective  $x_{36}$  value. Repulsion of  $\nu_3 + \nu_6$  by  $\nu_5$  in the opposite way is predicted for H<sub>3</sub>SnI, and since  $W_{356}$  is expected to be large ( $2-3$  cm<sup>-1</sup>), the discontinuous change of  $x_{36}$  going from H<sub>3</sub>SnCl to H<sub>3</sub>SnI finds a simple explanation.

Finally it should be noted that the excited state parameters of the stannyl halides are semiquantitatively in good agreement with those of the corresponding germlyl halides [5–7], and an analogy in the treatment of the higher-lying fundamentals of the stannyl halides may be expected.

#### Acknowledgement

We wish to thank the Deutsche Forschungsgemeinschaft for financial support through the Sonderforschungsbereich 42. Support by the Fonds der Chemie is gratefully acknowledged.

- [1] M. Betzel, H. Bürger, and P. Schulz, *Z. Naturforsch.* **39a**, 155 (1984).
- [2] H. Bürger and M. Betzel, *Z. Naturforsch.* **40a**, 989 (1985).
- [3] H. Bürger, P. Schulz, and J. Kauppinen, *J. Mol. Spectrosc.*, in the press.
- [4] J. Kauppinen, T. Kärkkäinen, and E. Kyrö, *J. Mol. Spectrosc.* **71**, 15 (1978).
- [5] H. Bürger, P. Schulz, and S. Cradock, *Z. Naturforsch.* **40a**, 383 (1985).
- [6] H. Bürger, R. Eujen, A. Rahner, and P. Schulz, *Z. Naturforsch.* **39a**, 871 (1984).
- [7] H. Bürger, R. Eujen, A. Rahner, P. Schulz, J. E. Drake, and S. Cradock, *Z. Naturforsch.* **38a**, 740 (1983).
- [8] G. J. Cartwright and I. M. Mills, *J. Mol. Spectrosc.* **34**, 415 (1970).
- [9] C. Betrencourt-Stirnermann, G. Graner, D. E. Jennings, and W. E. Blass, *J. Mol. Spectrosc.* **69**, 179 (1978).
- [10] L. C. Krisher, R. A. Gsell, and J. M. Bellama, *J. Chem. Phys.* **54**, 2287 (1971).
- [11] S. N. Wolf, L. C. Krisher, and R. A. Gsell, *J. Chem. Phys.* **54**, 4605 (1971).

- [12] S. N. Wolf, L. C. Krisher, and R. A. Gsell, *J. Chem. Phys.* **55**, 2106 (1971).
- [13] Lists of observed and calculated transition wave-numbers may be obtained from Fachinformationszentrum Energie – Physik – Mathematik, D-7514 Eggenstein-Leopoldshafen, West Germany, on submission of the name of the authors, the literature reference and the registry Nr. IRD-100 20.
- [14] M. Betzel, H. Bürger, and P. Schulz, to be published.
- [15] M. Morillon-Chapey, G. Guelachvili, and P. Jensen, *Canad. J. Phys.* **62**, 247 (1984).
- [16] F. Lattanzi, C. di Lauro, H. Bürger, and P. Schulz, *Mol. Phys.* **48**, 1209 (1983).
- [17] F. Lattanzi, C. di Lauro, H. Bürger, R. Eujen, P. Schulz, and S. Cradock, *Mol. Phys.* **51**, 81 (1984).